Published in final edited form as:
*NMR Biomed*. 2013 July ; 26(7): 756–765. doi:10.1002/nbm.2872.

# Multimodal Iron Oxide Nanoparticles for Hybrid Biomedical Imaging

**Timo Heidt**[a] and **Matthias Nahrendorf**[a,*]

[a]Center for Systems Biology, Massachusetts General Hospital and Harvard Medical School, Boston, Massachusetts

## Abstract

Iron oxide core nanoparticles are attractive imaging agents because their material properties allow the tuning of pharmacokinetics as well as attachment of multiple moieties to their surface. In addition to affinity ligands, these include fluorochromes and radioisotopes for detection with optical and nuclear imaging. As the iron oxide core can be detected by MRI, options for combining imaging modalities are manifold. Already, preclinical imaging strategies combine non-invasive imaging with higher resolution techniques such as intravital microscopy to gain unprecedented insight into steady state biology and disease. Going forward, hybrid iron oxide nanoparticles will likely help to merge modalities, creating a synergy that enables imaging in basic research and, potentially, also in the clinic.

### Keywords

nanoparticle; iron oxide; multimodality; multiscale; molecular imaging; MRI; PET; optical imaging

## Introduction

Advances in cellular and molecular imaging increasingly allow to study biology during steady state and disease in vivo. In addition to a deeper understanding of disease processes in basic research, these may also transform clinical practice. Tracking disease-promoting cells and molecules could lead to customized therapy and facilitate preventive medicine through personalized risk assessment. Two disease areas that create the biggest health burden in today's society dominate molecular imaging research: cardiovascular disease and cancer. Atherosclerosis is often detected when alterations in blood flow occur and heart muscle or brain tissue infarct -- a late stage of disease with irreversible organ damage. Similarly, many cancerous lesions have already progressed to advanced disease and spawned metastases at the time of detection, hindering curative therapy. Clinical molecular imaging may detect disease earlier, facilitate staging, monitor patient's recovery and assess treatment efficacy (1–4).

Nanoparticles comprise a key molecular imaging agent class. Often composites of different materials, their diameter is typically below 100nm. Among the manifold nanoparticles described, dextran coated iron oxide nanoparticles are proven work horses for multimodality preclinical imaging as they allow MRI as well as nuclear (PET, SPECT) and optical (fluorescence imaging) detection, if derivatized with appropriate beacons. While we have

*Correspondence: Matthias Nahrendorf, MD, PhD, Center for Systems Biology, 185 Cambridge Street, Boston, MA 02114, Telephone: (617) 643-0500, FAX: (617) 643-6133, mnahrendorf@mgh.harvard.edu.

seen numerous basic research applications, iron oxide core nanoparticles are not yet established in clinical practice, however, the number of promising translational studies with human patients is steadily growing (5–12). In this review we provide an overview on recent advances in multimodality/multiscale imaging while focussing on iron oxide-based nanoparticle-facilitated applications in preclinical and clinical imaging of cardiovascular disease and cancer.

## Nanoparticles

Nanoparticles have unique properties (these may be magnetic, optical or structural) that differ from either individual atoms or the bulk material (13–18). Various nanoparticle classes have been proposed for preclinical molecular targeting. Quantum dots for fluorescence imaging (19; 20), composites of iron oxides or gadolinium with silica or gold (21), micelles (22; 23), proteins (24) or dendrimers (25) have extensively been studied and are reviewed elsewhere (26–31).

In this review we will focus on derivatized dextran-coated magnetic nanoparticles with an iron oxide core. Growing experience with iron oxide nanoparticles over the last decades have influenced investigation and guided different methods of nanoparticle synthesis (e.g. microemulsions, hydrothermal reactions, sol-gel syntheses)(27). Superparamagnetic iron oxides are commonly produced using a precipitation method from alkaline solution containing a mixture of iron salts and a polymer coating to stabilize the compound in physiological solution (32–34). Tuning the surface coating may modify particle size and pharmacokinetics (35; 36). Dextran polymers, which are frequently used as coating materials, have previously been used in plasma expanders in the clinic (37). To prevent desorption of dextran from the iron oxide core, composites can be treated with epichlorhydrin to covalently cross-link the coating with the iron oxide core (cross-linked iron oxide nanoparticle, CLIO). Alternatively, carboxylated dextran can form the primary coating, a clinically viable alternative (5; 38; 39). Dextran coating provides for efficient conjugation chemistry through introduction of amines into the nanostructure (40). A high quantity of carboxylic or amine groups provides sufficient handles to label CLIO with affinity ligands or radioactive isotopes and fluorochromes for detection (Figure 1). Click chemistry (41–43), e.g. bioorthogonal cycloaddition reaction between 1,2,4,5-tetrazene and *trans*-cyclooctene (called “BOND” for bioorthogonal nanoparticle detection) (44; 45) can be used to rapidly add ligands. This may be particularly attractive for attachment of fast-decaying radioisotopes such as Fluorine-18 (46). If derivatized with appropriate affinity ligands, iron oxide particles can actively bind to targets. Alternatively, depending on the surface design, iron oxide nanoparticles are internalized by phagocytic or other cell types (47; 48). Phagocytes, including monocytes and macrophages, are often a focus of interest due to their key role in disease promotion. Suitable cell-specific nanoparticles can be identified with library approaches, in which their surface is randomly modified with small molecules. The fluorescence label allows for rapid screening of particle library uptake. This “trial and error” concept also facilitates nanoparticle selection with reduced phagocytic background uptake for targeting ligand strategies (49; 50). Further, libraries may be used to rapidly assess effects of nanoparticle toxicity (51).

## Imaging Techniques

### Magnetic resonance imaging

MRI is a modality with high spatial resolution and excellent soft tissue contrast (52). By adding molecular and cellular information to assessment of morphology, nanoparticles facilitate integration of anatomic, physiological and molecular data (53). The presence of iron oxide nanoparticles modulates proton spins, which is typically detected in $T_2$/$T_2$*-

weighted sequences, capitalizing on the strong $T_2$ relaxivity of the iron oxide core. While particles are not directly visualized, interaction with surrounding protons leads to powerful signal amplification. This concept has been applied to detect phagocytic cells in liver, spleen and lymph nodes (54–56) and in diseased tissues with phagocyte accumulation, such as vascular inflammation (57–62) or cancer (38; 63). The negative MRI contrast associated with iron oxide nanoparticles limits their use to target tissue with high initial signal and impairs the detection of the nanoparticle-specific signal decrease in the lung. Discrimination between nanoparticle-induced negative contrast and artifacts (e.g. air, motion, blood flow and interfaces with high susceptibility differences) can be difficult. Acquisition of pre- and post-injection images or positive contrast sequences for iron oxide detection, providing bright iron signals, address some of the technical challenges and improve specificity (64–68).

### Nuclear Imaging

Nuclear imaging is known for its high sensitivity ($10^{-10}$ to $10^{-12}$ mol/l), and its quantitative capabilities. Disadvantages are exposure to radiation, limited spatial resolution and the relative lack of anatomic detail. The latter is overcome by fusion of nuclear with anatomic imaging in hybrid techniques such as PET/CT or PET/MRI. For detection with nuclear imaging, nanoparticles are derivatized with radioisotopes such as Indium-111, Fluorine-18, Copper-64 or Zirconium-89. Often, this may be achieved by attachment of a chelator to the nanoparticle, and addition of the isotope just before injection (69). The ability to quantify very sparse targets with low doses of nanoparticles makes nuclear detection of nanoparticles highly attractive. Differences to detection by MRI are the positive and particle-specific increase in imaging signal.

### Optical Imaging

Fluorochromes have long played a major role in biotechnology by facilitating techniques such as histology, flow cytometry, and sequencing. Advantages are the versatility, multispectral capabilities, cost-effectiveness and sensitivity of optical detection. Fluorochromes such as indocyanine green are non-toxic and therefore qualify for human use. Expansion to the near infrared (NIR, 650–900 nm) spectrum overcame some of the limitations of optical imaging, including photon absorption, scattering, and background from endogenous tissue autofluorescence (70). Shifting to the NIR spectrum also allows deeper tissue penetration, and facilitated whole body tomography of rodents (71) and intravital microscopy of structures up to hundreds of micrometers within the tissue by confocal and multiphoton mode (72). The simplicity of planar fluorescence reflectance imaging (FRI) led to widespread research application, and clinical translation in endoscopic fluorescence imaging, intravascular fluorescence catheters or intraoperative fluorescence imaging is being explored (73–75). Tomographic fluorescence techniques (fluorescence molecular tomography, FMT) resolve the quantitative limitations of planar imaging and generate volumetric, three-dimensional maps of fluorochrome concentration (76). Here, fluorochrome-labeled nanoparticles can be detected and the concentration rapidly quantified with high sensitivity (77) while spectrally resolved fluorochromes enable multichannel imaging (78). In addition, upconverting nanoparticles containing rare earths such as yttrium oxide may be useful. These nanoparticles absorb light in the near infrared spectrum and emit their signal at shorter wave length, a phenomenon called Anti-Stokes emission (79; 80). The changed emission spectrum avoids tissue autofluorescence and improves specificity of detection.

### Miniaturized Detection Approaches (Diagnostic Magnetic Resonance - DMR Chip)

The use of labeled dextran-coated iron oxide nanoparticles as biosensors for diagnostic magnetic resonance is a relatively recent development for the ex vivo detection of analytes

(Figure 2) (81; 82). DMR devices, meant to be used at the point of care, employ magnetic nanoparticles for detection of DNA, proteins, receptors, cells, bacteria or toxins with high sensitivity. The devices resemble miniaturized MR systems, with a small permanent magnet and smart phones or tablets serving as the "console". For DMR, fluid samples of optically opaque test material (blood, sputum, biopsies) are incubated with nanoparticles that carry target-specific affinity ligands. By sensing changes in the $T_2$ relaxivity of the sample, the analyte can rapidly be detected, without the need of extensive sample processing. In clinical translation, DMR of human tumor tissue from fine needle aspirates was shown to provide accurate measures of multiple tumor markers in less than one hour, much faster than conventional histology techniques (83).

## Multimodality Imaging

Imaging modalities strongly vary in sensitivity, spatial and temporal resolution, and quantitative capabilities. An ideal imaging technique that maximizes all of the above has yet to be developed. To overcome specific modality limitations, multimodality imaging combines techniques with complementary strength. Co-registration of anatomical detail to physiological and molecular data allows exact signal localization and correlation to physiology (69; 84; 85). Theoretically, spectrally resolved fluorescence channels could be combined with MRI and radionuclide imaging to follow multiple distinct nanoparticle batches with different affinities, and hence molecular targets, simultaneously. We found that radionuclide and optical signals originating from the same nanoparticle correlate well between modalities (Figure 3) (86). Thus, while nuclear imaging of nanoparticles may be the most sensitive clinical route to translation, optical imaging could be used to accelerate preclinical development, minimizing the hurdles and costs associated with radioisotope handling. Fluorochromes do not decay like nuclear isotopes and provide convenient access to higher resolution agent localization techniques as FRI or fluorescence microscopy. Additionally, fluorochrome-derivatized nanoparticles can be detected by flow cytometry, which facilitates the quantitation of cellular uptake into specific cell populations identified by surface antigen expression (Figure 4).

## Multimodal Nanoparticles for Imaging of Atherosclerosis

The development of atherosclerosis is a chronic inflammatory multi-step process leading to vulnerable, rupture-prone plaques (87; 88). Hence, methods that elucidate immunobiological changes within the vessel wall may be suitable to detect a future culprit lesion (89). Molecular imaging has targeted early and late events in the inflammatory cascade of atherothrombosis (reviewed in 1; 77; 90; 91). Many preclinical and several clinical studies used nanoparticles to follow cardiovascular targets. If early disease events are of interest, one can detect vascular cell adhesion molecule-1 (VCAM-1) using affinity peptide-derivatized, fluorochrome-labeled iron oxide nanoparticles (CLIO-Cy5.5) (59). Targeting of oxidized LDL with lipid-coated iron oxide nanoparticles as well as gadolinium(Gd)/fluorescence-derivatized HDL facilitates detection of lipid rich atherosclerotic plaques in apolipoprotein E deficient ($apoE^{-/-}$) mice (92; 93).

Phagocytic myeloid cells, especially monocytes and macrophages, are key innate immune cells furnishing vascular wall inflammation. The detection and quantification of myeloid cell infiltration provides a valuable marker of inflammatory activity. Dextran-coated iron oxide nanoparticles, labeled nanocrystal-core HDL or affinity ligand derivatized Gd-immunomicelles are all avidly internalized into phagocytes and can be used to efficiently detect macrophage presence in atherosclerotic plaque with MR, optical and nuclear imaging techniques (69; 94; 95). Nanoparticle imaging with PET reduces the dose required for detection of inflammatory cells (60). Furthermore, fluorescent co-labeling enables the

localization of the nanoparticle to the atherosclerotic plaque and ultimately to the cellular source by ex vivo FRI, fluorescence microscopy or flow cytometry of vascular target tissue.

## Myocardial Infarction

Infarct healing and cardiac remodeling involve a complex set of interconnected cellular and molecular events, many of which are still incompletely understood. Visualization and in vivo detection of the underlying biology helps to understand the tissue changes after MI. Initially, ischemia leads to loss of cardiomyocytes due to necrosis and apoptosis. While necrotic cells are permanently lost, apoptosis is potentially reversible and thus a potential therapeutic target. Delayed Gd-DTPA enhancement MRI identifies the infarcted area, but cannot differentiate between necrotic and apoptotic cells. An annexin 5-labeled CLIO-Cy5.5 nanoparticle detected cardiomyocyte apoptosis early after myocardial infarction with high sensitivity using $T_2$* weighted MRI. Specificity of the signal was tested by co-localization on ex vivo fluorescence imaging (96; 97). Cell death next elicits a robust inflammatory response (98). Early neutrophil infiltration is followed by monocytes supplied by the bone marrow and the splenic reservoir (99). Inflammation seems essential for initiation of wound healing, while an excessive or insufficient inflammatory response may both be detrimental, leading to adverse remodeling, left ventricular dilation and heart failure (100). Thus, investigating inflammatory cell recruitment to the infarcted area (101), possibly in conjunction with other healing biomarkers like protease activity (78), could provide insight into biomarker networks. In a multi-channel MRI/FMT offline fusion approach, injection of fluorescent iron oxide nanoparticles allowed the monitoring of phagocytic recruitment to the myocardium (99). A co-injected cathepsin protease fluorescence sensor utilized a spectrally distinct channel on FMT to assess proteolytic activity induced by inflammatory cells. Ex vivo analysis then confirmed the source and location of the signal. In clinical practice, monitoring of infarct healing, for instance by MRI of iron oxide nanoparticle uptake into monocyte/macrophages recruited to the infarct scar shortly after the ischemic injury, could identify patients at risk and guide therapy that aims to prevent heart failure.

## Transplant Rejection

The ability to non-invasively image the pathophysiology of acute or chronic transplant rejection is an advance that promises to support clinical surveillance of grafts, which currently relies on repetitive tissue biopsies. For instance, radiolabeled antibodies detected cardiomyocyte injury (102). MRI combining biological (inflammation, cell injury) and functional (wall movement, ejection fraction) information would comprehensively assess a transplanted heart in one single investigation. Since phagocytes invade a rejecting organ, iron oxide particles can detect allograft rejection and would facilitate graft monitoring (103). A multimodality CLIO-Cy5.5 nanoparticle quantified phagocytosis during graft rejection, and was detected with MRI and FMT (104). A co-injected fluorescence protease-sensor additionally allowed the assessment of protease activity via a spectrally distinct FMT channel. Ex vivo analysis exploited the fluorescence label on the nanoparticle for FRI and flow cytometry to confirm macrophage uptake (104). Alternatively, Hitchens et al. investigated a $^{19}$F-fluorescence-labeled perfluorocarbon particle for macrophage infiltration of organ grafts by Fluorine-19 MRI (105). The advantage of this approach is the highly specific positive contrast created by the injected imaging agent, however, this may come with the cost of lower sensitivity.

## Aortic Aneurysms

Current guidelines recommend invasive repair for abdominal aortic aneurysms once the diameter exceeds 5.5 cm or the size progresses more than 1 cm/year (106). As most patients are asymptomatic and invasive aneurysm repair is associated with a high peri-operative mortality, the interest in alternative decision-making strategies is growing (107; 108).

Preclinical molecular imaging strategies now offer the assessment of the cellular and molecular pathobiology behind aneurysm formation and rupture. Infiltrating inflammatory cells secrete matrix metalloproteinases which promote degradation of extracellular matrix and compromise the integrity of the vascular wall. These inflammatory processes support the progression of aneurysms and ultimately cause aneurysm rupture (109). A CLIO platform labeled with the PET isotope Fluorine-18 and a fluorochrome was used in the apoE$^{-/-}$ mouse aneurysm model (46). PET/CT quantified macrophage infiltration in the vascular wall and may be a prognostic marker for aneurysm progression. The fluorescence label on the nanoparticle confirmed its cellular uptake profile by flow cytometry (46). Klink et al. used CNA-35 gadolinium micelles to image collagen in the wall of abdominal aortic aneurysm. Concomitant fluorescence labeling facilitated confirmation of target binding. With progression of aneurysm size, collagen loss in the aortic wall correlated to aneurysm "instability" and the likelihood to rupture (110). A recent clinical pilot study on iron oxide nanoparticle MRI in patients with aortic aneurysms demonstrated feasibility and showed promise for predicting aneurysm growth in the clinical setting (11). Ultimately, one could envision a clinical situation in which a large but biologically inactive aneurysm is not surgically treated but followed with watchful waiting, while smaller but highly inflamed aneurysms are treated aggressively. This may reduce both, rupture prevalence and surgery-related risk in stable patients.

### Cancer Inflammation and Cell Tracking

Cancer is associated with an inflammatory response of the innate and acquired immune system (111). Tumor cells recruit inflammatory cells which modulate the stroma, including extracellular matrix, and the tumor microenvironment. Infiltration of tumor associated macrophages (TAMs) promoting angiogenesis, invasion and metastasis represents a potential prognostic marker. We used CLIO-Cy5.5 to detect TAMs in murine cancer (112) and to explore co-localisation with additional biomarkers of inflammation (protease activity and integrins) using PET-FMT/CT (86). Others investigated iron oxide-fluorescence nanoemulsions of different sizes for uptake by tumor cells and TAMs (113). An alternative strategy is to image tumor cells directly via targeting of specific cell epitopes. Here, attachment of affinity ligands provides sensitivity for specific cancer cell lines (114–119). Targeting $\alpha_v\beta_3$ expression in murine cancer using magnetofluorescence (120; 121) or radiomagnetic (122) nanoparticles enabled the visualization of nanoparticle binding to integrin expressing cells with SPECT, PET, MRI and optical techniques (FMT, FRI or fluorescence microscopy) (120). Gianella et al. additionally incorporated glucocorticoids into a magnetofluorescent nanoemulsion platform for drug delivery (123). Furthermore, nanoparticles can also be applied for in vivo tracking of hematopoietic, possibly also neoplastic cells (124). Derivatization of the dextran coat with a membrane translocation signal (HIV-Tat peptide)(125) caused internalization of the nanoparticle, specifically into CD34+ cells, which was followed with MRI and fluorescence imaging.

## Clinical Studies

Clinical translation of complex multimodality nanoparticles faces considerable obstacles, including regulatory hurdles. One approach to clinical translation may be simplification of nanoparticle structures or the use of approved building blocks to better navigate regulatory concerns (126). Nevertheless, first imaging probes have passed the hurdle to clinical translation. Several studies investigated macrophage infiltration into inflamed atherosclerotic plaques (6–8). Trivedi et al. imaged symptomatic carotid stenosis of 30 patients scheduled for carotid endarterectomy with MRI before and after injection of iron oxide nanoparticles. Increased contrast was detected in 80% of the plaques and correlated significantly with histopathological data and staining for macrophages (9). Consequently, Patterson et al. applied iron oxide enhanced MRI to monitor the effects of statin treatment

on carotid plaque inflammation over a course of 12 weeks (10). High dose treatment resulted in significantly reduced MRI contrast, when compared to low dose statin therapy. Macrophage infiltration as a marker of inflammation of the vascular wall was followed in a clinical pilot study of abdominal aortic aneurysms. Richards et al. imaged 29 patients with aortic aneurysms before and after administration of iron oxide nanoparticles. Macrophages were detected in the aneurysm wall and iron oxide uptake into these cells was confirmed by histology. Interestingly, patients with higher nanoparticle uptake had significantly higher aneurysm growth rates, indicating the potential of this technique to guide clinical surveillance and treatment decisions (11). The idea to use nanoparticles for early detection and monitoring of disease is also supported by recent work by Gaglia et al. (39). The authors correlated MRI contrast changes after injection of iron oxide nanoparticles to insulitis in patients with recent-onset type 1 diabetes. As inflammatory phagocytes infiltrate pancreatic islets before the onset and with progression of diabetes, iron oxide nanoparticles could facilitate early detection of the disease and patient surveillance.

Molecular imaging has probably gained most clinical momentum in the early detection and staging of cancer. Harisinghani et. al. investigated 80 patients with prostate cancer and targeted phagocytic myeloid cells in lymph nodes with iron oxide nanoparticles. Using MRI, lymph node metastases were identified as areas that did not decrease in signal after nanoparticle injection, down to lesions of 2 mm in diameter (5). Comparison to surgical biopsies showed an excellent sensitivity and specificity. The use of ex vivo diagnostics that rely on nanoparticle detection (83) faces less hurdles for clinical translation and may therefore evolve rapidly.

## Summary

Multimodal protocols are already changing the way we image, and some of these advances are supported by hybrid nanoparticles. Nanoparticles that are detectable across modalities are frequently used for validation purposes. For instance, after in vivo nuclear or magnetic resonance imaging, fluorescence serves to pinpoint the nanoparticle signal to specific tissues, cells and molecular targets. Further, nanoparticles with multiple detection options are used in multiscale experiments, in which targets are followed non-invasively first, and subsequently with higher resolution techniques such as intravital fluorescence microscopy or flow cytometry. The combination of different scales connects non-invasive with potentially more specific invasively gained data, and thus facilitates insight into complex basic biology. Finally, multiscale imaging may enhance clinical diagnostics in the near future. A hypothetical application could be the non-invasive whole body detection of nanoparticles by PET (in inflamed atherosclerotic plaque or tumors), which could be followed by real-time optical visualization of particle deposition during invasive therapeutic procedures. These could include local detection of inflammatory plaque by intravascular fluorescence-sensing wires (127) during stent implantation, or detection of tumor margins by intra-operative fluorescence imaging (128; 129). Future work will provide additional proof-of-concept and hopefully clinical data in support of these concepts.

## Acknowledgments

This work was funded in parts by grants from the NIH (R01HL095629, R01HL096576, Translational Program of Excellence in Nanotechnology HHSN268201000044C) and DFG (HE6382/1-1).

## Abbreviations

**BOND** Bioorthogonal Nanoparticle Detection

| | |
|---|---|
| **CLIO** | Cross Linked Iron Oxide |
| **CT** | Computed Tomography |
| **Cy5.5** | Cyanine 5.5 |
| **DMR** | Diagnostic Magnetic Resonance |
| **FM** | Fluorescence Microscopy |
| **FMT** | Fluorescence Molecular Tomography |
| **FRI** | Fluorescence Reflectance Imaging |
| **Gd** | Gadolinium |
| **HDL** | High Density Lipoprotein |
| **LDL** | Low Density Lipoprotein |
| **LV** | Left Ventricle |
| **MRI** | Magnetic Resonance Imaging |
| **NIR** | Near-InfraRed |
| **TAM** | Tumor Associated Macrophages |

## References


1. Sanz J, Fayad ZA. Imaging of atherosclerotic cardiovascular disease. Nature. 2008; 451:953–957. [PubMed: 18288186]
2. Massoud TF, Gambhir SS. Molecular imaging in living subjects: seeing fundamental biological processes in a new light. Genes Dev. 2003; 17:545–580. [PubMed: 12629038]
3. Weissleder R, Pittet MJ. Imaging in the era of molecular oncology. Nature. 2008; 452:580–589. [PubMed: 18385732]
4. Leuschner F, Nahrendorf M. Molecular imaging of coronary atherosclerosis and myocardial infarction: considerations for the bench and perspectives for the clinic. Circ Res. 2011; 108:593–606. [PubMed: 21372291]
5. Harisinghani MG, Barentsz J, Hahn PF, Deserno WM, Tabatabaei S, van de Kaa CH, de la Rosette J, Weissleder R. Noninvasive detection of clinically occult lymph-node metastases in prostate cancer. N Engl J Med. 2003; 348:2491–2499. [PubMed: 12815134]
6. Schmitz SA, Taupitz M, Wagner S, Wolf KJ, Beyersdorff D, Hamm B. Magnetic resonance imaging of atherosclerotic plaques using superparamagnetic iron oxide particles. J Magn Reson Imaging. 2001; 14:355–361. [PubMed: 11599058]
7. Kooi ME, Cappendijk VC, Cleutjens KB, Kessels AG, Kitslaar PJ, Borgers M, Frederik PM, Daemen MJ, van Engelshoven JM. Accumulation of ultrasmall superparamagnetic particles of iron oxide in human atherosclerotic plaques can be detected by in vivo magnetic resonance imaging. Circulation. 2003; 107:2453–2458. [PubMed: 12719280]
8. Tang TY, Howarth SP, Li ZY, Miller SR, Graves MJ, U-King-Im JM, Trivedi RA, Walsh SR, Brown AP, Kirkpatrick PJ, Gaunt ME, Gillard JH. Correlation of carotid atheromatous plaque inflammation with biomechanical stress: utility of USPIO enhanced MR imaging and finite element analysis. Atherosclerosis. 2008; 196:879–887. [PubMed: 17350023]
9. Trivedi RA, Mallawarachi C, U-King-Im JM, Graves MJ, Horsley J, Goddard MJ, Brown A, Wang L, Kirkpatrick PJ, Brown J, Gillard JH. Identifying inflamed carotid plaques using in vivo USPIO-enhanced MR imaging to label plaque macrophages. Arterioscler Thromb Vasc Biol. 2006; 26:1601–1606. [PubMed: 16627809]
10. Patterson AJ, Tang TY, Graves MJ, Muller KH, Gillard JH. In vivo carotid plaque MRI using quantitative T2* measurements with ultrasmall superparamagnetic iron oxide particles: a dose-response study to statin therapy. NMR Biomed. 2011; 24:89–95. [PubMed: 21259368]

11. Richards JM, Semple SI, MacGillivray TJ, Gray C, Langrish JP, Williams M, Dweck M, Wallace W, McKillop G, Chalmers RT, Garden OJ, Newby DE. Abdominal aortic aneurysm growth predicted by uptake of ultrasmall superparamagnetic particles of iron oxide: a pilot study. Circ Cardiovasc Imaging. 2011; 4:274–281. [PubMed: 21304070]
12. Richards JM, Shaw CA, Lang NN, Williams MC, Semple SI, Macgillivray TJ, Gray C, Crawford JH, Alam SR, Atkinson AP, Forrest EK, Bienek C, Mills NL, Burdess A, Dhaliwal K, Simpson AJ, Wallace WA, Hill AT, Roddie PH, McKillop G, Connolly TA, Feuerstein GZ, Barclay GR, Turner ML, Newby DE. In vivo mononuclear cell tracking using superparamagnetic particles of iron oxide: feasibility and safety in humans. Circ Cardiovasc Imaging. 2012; 5:509–517. [PubMed: 22787016]
13. Jarzyna PA, Gianella A, Skajaa T, Knudsen G, Deddens LH, Cormode DP, Fayad ZA, Mulder WJ. Multifunctional imaging nanoprobes. Wiley Interdiscip Rev Nanomed Nanobiotechnol. 2010; 2:138–150. [PubMed: 20039335]
14. Pan D, Carauthers SD, Chen J, Winter PM, SenPan A, Schmieder AH, Wickline SA, Lanza GM. Nanomedicine strategies for molecular targets with MRI and optical imaging. Future Med Chem. 2010; 2:471–490. [PubMed: 20485473]
15. Kim BY, Rutka JT, Chan WC. Nanomedicine. N Engl J Med. 2010; 363:2434–2443. [PubMed: 21158659]
16. Xie J, Lee S, Chen X. Nanoparticle-based theranostic agents. Adv Drug Deliv Rev. 2010; 62:1064–1079. [PubMed: 20691229]
17. Sosnovik DE, Nahrendorf M, Weissleder R. Magnetic nanoparticles for MR imaging: agents, techniques and cardiovascular applications. Basic Res Cardiol. 2008; 103:122–130. [PubMed: 18324368]
18. Stephen ZR, Kievit FM, Zhang M. Magnetite Nanoparticles for Medical MR Imaging. Mater Today (Kidlington). 2011; 14:330–338. [PubMed: 22389583]
19. Alivisatos P. The use of nanocrystals in biological detection. Nat Biotechnol. 2004; 22:47–52. [PubMed: 14704706]
20. Stroh M, Zimmer JP, Duda DG, Levchenko TS, Cohen KS, Brown EB, Scadden DT, Torchilin VP, Bawendi MG, Fukumura D, Jain RK. Quantum dots spectrally distinguish multiple species within the tumor milieu in vivo. Nat Med. 2005; 11:678–682. [PubMed: 15880117]
21. van Schooneveld MM, Cormode DP, Koole R, van Wijngaarden JT, Calcagno C, Skajaa T, Hilhorst J, ‘t Hart DC, Fayad ZA, Mulder WJ, Meijerink A. A fluorescent, paramagnetic and PEGylated gold/silica nanoparticle for MRI CT and fluorescence imaging. Contrast Media Mol Imaging. 2010; 5:231–236. [PubMed: 20812290]
22. Briley-Saebo KC, Amirbekian V, Mani V, Aguinaldo JG, Vucic E, Carpenter D, Amirbekian S, Fayad ZA. Gadolinium mixed-micelles: effect of the amphiphile on in vitro and in vivo efficacy in apolipoprotein E knockout mouse models of atherosclerosis. Magn Reson Med. 2006; 56:1336–1346. [PubMed: 17089381]
23. Nitin N, LaConte LE, Zurkiya O, Hu X, Bao G. Functionalization and peptide-based delivery of magnetic nanoparticles as an intracellular MRI contrast agent. J Biol Inorg Chem. 2004; 9:706–712. [PubMed: 15232722]
24. Wilhelm C, Billotey C, Roger J, Pons JN, Bacri JC, Gazeau F. Intracellular uptake of anionic superparamagnetic nanoparticles as a function of their surface coating. Biomaterials. 2003; 24:1001–1011. [PubMed: 12504522]
25. Bulte JW, Douglas T, Witwer B, Zhang SC, Strable E, Lewis BK, Zywicke H, Miller B, van Gelderen P, Moskowitz BM, Duncan ID, Frank JA. Magnetodendrimers allow endosomal magnetic labeling and in vivo tracking of stem cells. Nat Biotechnol. 2001; 19:1141–1147. [PubMed: 11731783]
26. Lobatto ME, Fuster V, Fayad ZA, Mulder WJ. Perspectives and opportunities for nanomedicine in the management of atherosclerosis. Nat Rev Drug Discov. 2011; 10:835–852. [PubMed: 22015921]
27. Laurent S, Forge D, Port M, Roch A, Robic C, Vander Elst L, Muller RN. Magnetic iron oxide nanoparticles: synthesis, stabilization, vectorization, physicochemical characterizations, and biological applications. Chem Rev. 2008; 108:2064–2110. [PubMed: 18543879]

28. Michalet X, Pinaud FF, Bentolila LA, Tsay JM, Doose S, Li JJ, Sundaresan G, Wu AM, Gambhir SS, Weiss S. Quantum dots for live cells, in vivo imaging, and diagnostics. Science. 2005; 307:538–544. [PubMed: 15681376]
29. Li ZH, Peng J, Chen HL. Bioconjugated quantum dots as fluorescent probes for biomedical imaging. J Nanosci Nanotechnol. 2011; 11:7521–7536. [PubMed: 22097457]
30. Wei S, Wang Q, Zhu J, Sun L, Lin H, Guo Z. Multifunctional composite core-shell nanoparticles. Nanoscale. 2011; 3:4474–4502. [PubMed: 21984390]
31. Mahmoudi M, Serpooshan V, Laurent S. Engineered nanoparticles for biomolecular imaging. Nanoscale. 2011; 3:3007–3026. [PubMed: 21717012]
32. Tassa C, Shaw SY, Weissleder R. Dextran-coated iron oxide nanoparticles: a versatile platform for targeted molecular imaging, molecular diagnostics, and therapy. Acc Chem Res. 2011; 44:842–852. [PubMed: 21661727]
33. Weissleder R, Moore A, Mahmood U, Bhorade R, Benveniste H, Chiocca EA, Basilion JP. In vivo magnetic resonance imaging of transgene expression. Nat Med. 2000; 6:351–355. [PubMed: 10700241]
34. Devaraj NK, Keliher EJ, Thurber GM, Nahrendorf M, Weissleder R. 18F labeled nanoparticles for in vivo PET-CT imaging. Bioconjug Chem. 2009; 20:397–401. [PubMed: 19138113]
35. Veiseh O, Gunn JW, Zhang M. Design and fabrication of magnetic nanoparticles for targeted drug delivery and imaging. Adv Drug Deliv Rev. 2010; 62:284–304. [PubMed: 19909778]
36. Weissleder R, Elizondo G, Wittenberg J, Rabito CA, Bengele HH, Josephson L. Ultrasmall superparamagnetic iron oxide: characterization of a new class of contrast agents for MR imaging. Radiology. 1990; 175:489–493. [PubMed: 2326474]
37. Shen T, Weissleder R, Papisov M, Bogdanov AJ, Brady TJ. Monocrystalline iron oxide nanocompounds (MION): physicochemical properties. Magn Reson Med. 1993; 29:599–604. [PubMed: 8505895]
38. Harisinghani M, Ross RW, Guimaraes AR, Weissleder R. Utility of a new bolus-injectable nanoparticle for clinical cancer staging. Neoplasia. 2007; 9:1160–1165. [PubMed: 18084623]
39. Gaglia JL, Guimaraes AR, Harisinghani M, Turvey SE, Jackson R, Benoist C, Mathis D, Weissleder R. Noninvasive imaging of pancreatic islet inflammation in type 1A diabetes patients. J Clin Invest. 2011; 121:442–445. [PubMed: 21123946]
40. Weissleder R, Rehemtulla A, Gambhir S. Molecular Imaging - Principles and Practice. Pmph Usa. 2010
41. Shao F, Weissleder R, Hilderbrand SA. Monofunctional carbocyanine dyes for bio- and bioorthogonal conjugation. Bioconjug Chem. 2008; 19:2487–2491. [PubMed: 19053316]
42. Sun EY, Josephson L, Weissleder R. “Clickable” nanoparticles for targeted imaging. Mol Imaging. 2006; 5:122–128. [PubMed: 16954026]
43. Karver MR, Weissleder R, Hilderbrand SA. Bioorthogonal reaction pairs enable simultaneous, selective, multi-target imaging. Angew Chem Int Ed Engl. 2012; 51:920–922. [PubMed: 22162316]
44. Haun JB, Devaraj NK, Hilderbrand SA, Lee H, Weissleder R. Bioorthogonal chemistry amplifies nanoparticle binding and enhances the sensitivity of cell detection. Nat Nanotechnol. 2010; 5:660–665. [PubMed: 20676091]
45. Haun JB, Devaraj NK, Marinelli BS, Lee H, Weissleder R. Probing intracellular biomarkers and mediators of cell activation using nanosensors and bioorthogonal chemistry. ACS Nano. 2011; 5:3204–3213. [PubMed: 21351804]
46. Nahrendorf M, Keliher E, Marinelli B, Leuschner F, Robbins CS, Gerszten RE, Pittet MJ, Swirski FK, Weissleder R. Detection of macrophages in aortic aneurysms by nanoparticle positron emission tomography-computed tomography. Arterioscler Thromb Vasc Biol. 2011; 31:750–757. [PubMed: 21252070]
47. Josephson L, Kircher MF, Mahmood U, Tang Y, Weissleder R. Near-infrared fluorescent nanoparticles as combined MR/optical imaging probes. Bioconjug Chem. 2002; 13:554–560. [PubMed: 12009946]
48. Cormode DP, Skajaa GO, Delshad A, Parker N, Jarzyna PA, Calcagno C, Galper MW, Skajaa T, Briley-Saebo KC, Bell HM, Gordon RE, Fayad ZA, Woo SL, Mulder WJ. A versatile and tunable

coating strategy allows control of nanocrystal delivery to cell types in the liver. Bioconjug Chem. 2011; 22:353–361. [PubMed: 21361312]

49. Weissleder R, Kelly K, Sun EY, Shtatland T, Josephson L. Cell-specific targeting of nanoparticles by multivalent attachment of small molecules. Nat Biotechnol. 2005; 23:1418–1423. [PubMed: 16244656]
50. Kelly KA, Shaw SY, Nahrendorf M, Kristoff K, Aikawa E, Schreiber SL, Clemons PA, Weissleder R. Unbiased discovery of in vivo imaging probes through in vitro profiling of nanoparticle libraries. Integr Biol (Camb). 2009; 1:311–317. [PubMed: 20023731]
51. Shaw SY, Westly EC, Pittet MJ, Subramanian A, Schreiber SL, Weissleder R. Perturbational profiling of nanomaterial biologic activity. Proc Natl Acad Sci U S A. 2008; 105:7387–7392. [PubMed: 18492802]
52. Sinusas AJ, Bengel F, Nahrendorf M, Epstein FH, Wu JC, Villanueva FS, Fayad ZA, Gropler RJ. Multimodality cardiovascular molecular imaging, part I. Circ Cardiovasc Imaging. 2008; 1:244–256. [PubMed: 19808549]
53. Caruthers SD, Winter PM, Wickline SA, Lanza GM. Targeted magnetic resonance imaging contrast agents. Methods Mol Med. 2006; 124:387–400. [PubMed: 16506431]
54. Shamsi K, Balzer T, Saini S, Ros PR, Nelson RC, Carter EC, Tollerfield S, Niendorf HP. Superparamagnetic iron oxide particles (SH U 555 A): evaluation of efficacy in three doses for hepatic MR imaging. Radiology. 1998; 206:365–371. [PubMed: 9457187]
55. Weissleder R, Hahn PF, Stark DD, Elizondo G, Saini S, Todd LE, Wittenberg J, Ferrucci JT. Superparamagnetic iron oxide: enhanced detection of focal splenic tumors with MR imaging. Radiology. 1988; 169:399–403. [PubMed: 3174987]
56. Weissleder R, Stark DD, Rummeny EJ, Compton CC, Ferrucci JT. Splenic lymphoma: ferrite-enhanced MR imaging in rats. Radiology. 1988; 166:423–430. [PubMed: 3336717]
57. Briley-Saebo KC, Shaw PX, Mulder WJ, Choi SH, Vucic E, Aguinaldo JG, Witztum JL, Fuster V, Tsimikas S, Fayad ZA. Targeted molecular probes for imaging atherosclerotic lesions with magnetic resonance using antibodies that recognize oxidation-specific epitopes. Circulation. 2008; 117:3206–3215. [PubMed: 18541740]
58. Nahrendorf M, Keliher E, Panizzi P, Zhang H, Hembrador S, Figueiredo JL, Aikawa E, Kelly K, Libby P, Weissleder R. 18F-4V for PET-CT imaging of VCAM-1 expression in atherosclerosis. JACC Cardiovasc Imaging. 2009; 2:1213–1222. [PubMed: 19833312]
59. Nahrendorf M, Jaffer FA, Kelly KA, Sosnovik DE, Aikawa E, Libby P, Weissleder R. Noninvasive vascular cell adhesion molecule-1 imaging identifies inflammatory activation of cells in atherosclerosis. Circulation. 2006; 114:1504–1511. [PubMed: 17000904]
60. Nahrendorf M, Waterman P, Thurber G, Groves K, Rajopadhye M, Panizzi P, Marinelli B, Aikawa E, Pittet MJ, Swirski FK, Weissleder R. Hybrid in vivo FMT-CT imaging of protease activity in atherosclerosis with customized nanosensors. Arterioscler Thromb Vasc Biol. 2009; 29:1444–1451. [PubMed: 19608968]
61. Zhang J, Nie L, Razavian M, Ahmed M, Dobrucki LW, Asadi A, Edwards DS, Azure M, Sinusas AJ, Sadeghi MM. Molecular imaging of activated matrix metalloproteinases in vascular remodeling. Circulation. 2008; 118:1953–1960. [PubMed: 18936327]
62. Chen J, Tung CH, Mahmood U, Ntziachristos V, Gyurko R, Fishman MC, Huang PL, Weissleder R. In vivo imaging of proteolytic activity in atherosclerosis. Circulation. 2002; 105:2766–2771. [PubMed: 12057992]
63. Gianella A, Jarzyna PA, Mani V, Ramachandran S, Calcagno C, Tang J, Kann B, Dijk WJ, Thijssen VL, Griffioen AW, Storm G, Fayad ZA, Mulder WJ. Multifunctional nanoemulsion platform for imaging guided therapy evaluated in experimental cancer. ACS Nano. 2011; 5:4422–4433. [PubMed: 21557611]
64. Seppenwoolde JH, Viergever MA, Bakker CJ. Passive tracking exploiting local signal conservation: the white marker phenomenon. Magn Reson Med. 2003; 50:784–790. [PubMed: 14523965]
65. Farrar CT, Dai G, Novikov M, Rosenzweig A, Weissleder R, Rosen BR, Sosnovik DE. Impact of field strength and iron oxide nanoparticle concentration on the linearity and diagnostic accuracy of off-resonance imaging. NMR Biomed. 2008; 21:453–463. [PubMed: 17918777]

66. Cunningham CH, Arai T, Yang PC, McConnell MV, Pauly JM, Conolly SM. Positive contrast magnetic resonance imaging of cells labeled with magnetic nanoparticles. Magn Reson Med. 2005; 53:999–1005. [PubMed: 15844142]
67. Mani V, Briley-Saebo KC, Itskovich VV, Samber DD, Fayad ZA. Gradient echo acquisition for superparamagnetic particles with positive contrast (GRASP): sequence characterization in membrane and glass superparamagnetic iron oxide phantoms at 1.5T and 3T. Magn Reson Med. 2006; 55:126–135. [PubMed: 16342148]
68. Korosoglou G, Shah S, Vonken EJ, Gilson WD, Schar M, Tang L, Kraitchman DL, Boston RC, Sosnovik DE, Weiss RG, Weissleder R, Stuber M. Off-resonance angiography: a new method to depict vessels--phantom and rabbit studies. Radiology. 2008; 249:501–509. [PubMed: 18780823]
69. Nahrendorf M, Zhang H, Hembrador S, Panizzi P, Sosnovik DE, Aikawa E, Libby P, Swirski FK, Weissleder R. Nanoparticle PET-CT imaging of macrophages in inflammatory atherosclerosis. Circulation. 2008; 117:379–387. [PubMed: 18158358]
70. Weissleder R, Ntziachristos V. Shedding light onto live molecular targets. Nat Med. 2003; 9:123–128. [PubMed: 12514725]
71. Ntziachristos V. Fluorescence molecular imaging. Annu Rev Biomed Eng. 2006; 8:1–33. [PubMed: 16834550]
72. Pittet MJ, Weissleder R. Intravital imaging. Cell. 2011; 147:983–991. [PubMed: 22118457]
73. Sheth RA, Upadhyay R, Weissleder R, Mahmood U. Real-time multichannel imaging framework for endoscopy, catheters, and fixed geometry intraoperative systems. Mol Imaging. 2007; 6:147–155. [PubMed: 17532881]
74. Calfon MA, Vinegoni C, Ntziachristos V, Jaffer FA. Intravascular near-infrared fluorescence molecular imaging of atherosclerosis: toward coronary arterial visualization of biologically high-risk plaques. J Biomed Opt. 2010; 15 011107.
75. Sevick-Muraca EM. Translation of near-infrared fluorescence imaging technologies: emerging clinical applications. Annu Rev Med. 2012; 63:217–231. [PubMed: 22034868]
76. Ntziachristos V, Bremer C, Graves EE, Ripoll J, Weissleder R. In vivo tomographic imaging of near-infrared fluorescent probes. Mol Imaging. 2002; 1:82–88. [PubMed: 12920848]
77. Nahrendorf M, Sosnovik DE, French BA, Swirski FK, Bengel F, Sadeghi MM, Lindner JR, Wu JC, Kraitchman DL, Fayad ZA, Sinusas AJ. Multimodality cardiovascular molecular imaging, Part II. Circ Cardiovasc Imaging. 2009; 2:56–70. [PubMed: 19808565]
78. Leuschner F, Rauch PJ, Ueno T, Gorbatov R, Marinelli B, Lee WW, Dutta P, Wei Y, Robbins C, Iwamoto Y, Sena B, Chudnovskiy A, Panizzi P, Keliher E, Higgins JM, Libby P, Moskowitz MA, Pittet MJ, Swirski FK, Weissleder R, Nahrendorf M. Rapid monocyte kinetics in acute myocardial infarction are sustained by extramedullary monocytopoiesis. J Exp Med. 2012; 209:123–137. [PubMed: 22213805]
79. Salthouse C, Hildebrand S, Weissleder R, Mahmood U. Design and demonstration of a small-animal up-conversion imager. Opt Express. 2008; 16:21731–21737. [PubMed: 19104605]
80. Kuningas K, Pakkila H, Ukonaho T, Rantanen T, Lovgren T, Soukka T. Upconversion fluorescence enables homogeneous immunoassay in whole blood. Clin Chem. 2007; 53:145–146. [PubMed: 17202501]
81. Shao H, Min C, Issadore D, Liong M, Yoon TJ, Weissleder R, Lee H. Magnetic Nanoparticles and microNMR for Diagnostic Applications. Theranostics. 2012; 2:55–65. [PubMed: 22272219]
82. Lee H, Sun E, Ham D, Weissleder R. Chip-NMR biosensor for detection and molecular analysis of cells. Nat Med. 2008; 14:869–874. [PubMed: 18607350]
83. Haun JB, Castro CM, Wang R, Peterson VM, Marinelli BS, Lee H, Weissleder R. Micro-NMR for rapid molecular analysis of human tumor samples. Sci Transl Med. 2011; 3 71ra16.
84. Sosnovik DE, Nahrendorf M, Weissleder R. Molecular magnetic resonance imaging in cardiovascular medicine. Circulation. 2007; 115:2076–2086. [PubMed: 17438163]
85. Wu JC, Bengel FM, Gambhir SS. Cardiovascular molecular imaging. Radiology. 2007; 244:337–355. [PubMed: 17592037]
86. Nahrendorf M, Keliher E, Marinelli B, Waterman P, Feruglio PF, Fexon L, Pivovarov M, Swirski FK, Pittet MJ, Vinegoni C, Weissleder R. Hybrid PET-optical imaging using targeted probes. Proc Natl Acad Sci U S A. 2010; 107:7910–7915. [PubMed: 20385821]

87. Libby P. Inflammation in atherosclerosis. Nature. 2002; 420:868–874. [PubMed: 12490960]
88. Ross R. Atherosclerosis--an inflammatory disease. N Engl J Med. 1999; 340:115–126. [PubMed: 9887164]
89. Alsheikh-Ali AA, Kitsios GD, Balk EM, Lau J, Ip S. The vulnerable atherosclerotic plaque: scope of the literature. Ann Intern Med. 2010; 153:387–395. [PubMed: 20713770]
90. Buxton DB, Antman M, Danthi N, Dilsizian V, Fayad ZA, Garcia MJ, Jaff MR, Klimas M, Libby P, Nahrendorf M, Sinusas AJ, Wickline SA, Wu JC, Bonow RO, Weissleder R. Report of the National Heart, Lung, and Blood Institute working group on the translation of cardiovascular molecular imaging. Circulation. 2011; 123:2157–2163. [PubMed: 21576680]
91. Wu JC, Bengel FM, Gambhir SS. Cardiovascular molecular imaging. Radiology. 2007; 244:337–355. [PubMed: 17592037]
92. Briley-Saebo KC, Cho YS, Shaw PX, Ryu SK, Mani V, Dickson S, Izadmehr E, Green S, Fayad ZA, Tsimikas S. Targeted iron oxide particles for in vivo magnetic resonance detection of atherosclerotic lesions with antibodies directed to oxidation-specific epitopes. J Am Coll Cardiol. 2011; 57:337–347. [PubMed: 21106318]
93. Cormode DP, Briley-Saebo KC, Mulder WJ, Aguinaldo JG, Barazza A, Ma Y, Fisher EA, Fayad ZA. An ApoA-I mimetic peptide high-density-lipoprotein-based MRI contrast agent for atherosclerotic plaque composition detection. Small. 2008; 4:1437–1444. [PubMed: 18712752]
94. Amirbekian V, Lipinski MJ, Briley-Saebo KC, Amirbekian S, Aguinaldo JG, Weinreb DB, Vucic E, Frias JC, Hyafil F, Mani V, Fisher EA, Fayad ZA. Detecting and assessing macrophages in vivo to evaluate atherosclerosis noninvasively using molecular MRI. Proc Natl Acad Sci U S A. 2007; 104:961–966. [PubMed: 17215360]
95. Cormode DP, Skajaa T, van Schooneveld MM, Koole R, Jarzyna P, Lobatto ME, Calcagno C, Barazza A, Gordon RE, Zanzonico P, Fisher EA, Fayad ZA, Mulder WJ. Nanocrystal core high-density lipoproteins: a multimodality contrast agent platform. Nano Lett. 2008; 8:3715–3723. [PubMed: 18939808]
96. Sosnovik DE, Garanger E, Aikawa E, Nahrendorf M, Figuiredo JL, Dai G, Reynolds F, Rosenzweig A, Weissleder R, Josephson L. Molecular MRI of cardiomyocyte apoptosis with simultaneous delayed-enhancement MRI distinguishes apoptotic and necrotic myocytes in vivo: potential for midmyocardial salvage in acute ischemia. Circ Cardiovasc Imaging. 2009; 2:460–467. [PubMed: 19920044]
97. Sosnovik DE, Nahrendorf M, Panizzi P, Matsui T, Aikawa E, Dai G, Li L, Reynolds F, Dorn GWn, Weissleder R, Josephson L, Rosenzweig A. Molecular MRI detects low levels of cardiomyocyte apoptosis in a transgenic model of chronic heart failure. Circ Cardiovasc Imaging. 2009; 2:468–475. [PubMed: 19920045]
98. Frangogiannis NG. Regulation of the inflammatory response in cardiac repair. Circ Res. 2012; 110:159–173. [PubMed: 22223212]
99. Swirski FK, Nahrendorf M, Etzrodt M, Wildgruber M, Cortez-Retamozo V, Panizzi P, Figueiredo JL, Kohler RH, Chudnovskiy A, Waterman P, Aikawa E, Mempel TR, Libby P, Weissleder R, Pittet MJ. Identification of splenic reservoir monocytes and their deployment to inflammatory sites. Science. 2009; 325:612–616. [PubMed: 19644120]
100. Nahrendorf M, Pittet MJ, Swirski FK. Monocytes: protagonists of infarct inflammation and repair after myocardial infarction. Circulation. 2010; 121:2437–2445. [PubMed: 20530020]
101. Sosnovik DE, Nahrendorf M, Deliolanis N, Novikov M, Aikawa E, Josephson L, Rosenzweig A, Weissleder R, Ntziachristos V. Fluorescence tomography and magnetic resonance imaging of myocardial macrophage infiltration in infarcted myocardium in vivo. Circulation. 2007; 115:1384–1391. [PubMed: 17339546]
102. Narula J, Acio ER, Narula N, Samuels LE, Fyfe B, Wood D, Fitzpatrick JM, Raghunath PN, Tomaszewski JE, Kelly C, Steinmetz N, Green A, Tait JF, Leppo J, Blankenberg FG, Jain D, Strauss HW. Annexin-V imaging for noninvasive detection of cardiac allograft rejection. Nat Med. 2001; 7:1347–1352. [PubMed: 11726976]
103. Wu YL, Ye Q, Sato K, Foley LM, Hitchens TK, Ho C. Noninvasive evaluation of cardiac allograft rejection by cellular and functional cardiac magnetic resonance. JACC Cardiovasc Imaging. 2009; 2:731–741. [PubMed: 19520344]

104. Christen T, Nahrendorf M, Wildgruber M, Swirski FK, Aikawa E, Waterman P, Shimizu K, Weissleder R, Libby P. Molecular imaging of innate immune cell function in transplant rejection. Circulation. 2009; 119:1925–1932. [PubMed: 19332470]

105. Hitchens TK, Ye Q, Eytan DF, Janjic JM, Ahrens ET, Ho C. 19F MRI detection of acute allograft rejection with in vivo perfluorocarbon labeling of immune cells. Magn Reson Med. 2011; 65:1144–1153. [PubMed: 21305593]

106. Hirsch AT, Haskal ZJ, Hertzer NR, Bakal CW, Creager MA, Halperin JL, Hiratzka LF, Murphy WR, Olin JW, Puschett JB, Rosenfield KA, Sacks D, Stanley JC, Taylor LMJ, White CJ, White J, White RA, Antman EM, Smith SCJ, Adams CD, Anderson JL, Faxon DP, Fuster V, Gibbons RJ, Hunt SA, Jacobs AK, Nishimura R, Ornato JP, Page RL, Riegel B. ACC/AHA Guidelines for the Management of Patients with Peripheral Arterial Disease (lower extremity, renal, mesenteric, and abdominal aortic): a collaborative report from the American Associations for Vascular Surgery/Society for Vascular Surgery, Society for Cardiovascular Angiography and Interventions, Society for Vascular Medicine and Biology, Society of Interventional Radiology, and the ACC/AHA Task Force on Practice Guidelines (writing committee to develop guidelines for the management of patients with peripheral arterial disease)--summary of recommendations. J Vasc Interv Radiol. 2006; 17:1383–1397. quiz 1398. [PubMed: 16990459]

107. Sakalihasan N, Limet R, Defawe OD. Abdominal aortic aneurysm. Lancet. 2005; 365:1577–1589. [PubMed: 15866312]

108. DB B. Molecular imaging of aortic aneurysms. Circ Cardiovasc Imaging. 2012; 5:392–399. [PubMed: 22592009]

109. Shimizu K, Mitchell RN, Libby P. Inflammation and cellular immune responses in abdominal aortic aneurysms. Arterioscler Thromb Vasc Biol. 2006; 26:987–994. [PubMed: 16497993]

110. Klink A, Heynens J, Herranz B, Lobatto ME, Arias T, Sanders HM, Strijkers GJ, Merkx M, Nicolay K, Fuster V, Tedgui A, Mallat Z, Mulder WJ, Fayad ZA. In vivo characterization of a new abdominal aortic aneurysm mouse model with conventional and molecular magnetic resonance imaging. J Am Coll Cardiol. 2011; 58:2522–2530. [PubMed: 22133853]

111. Mantovani A, Allavena P, Sica A, Balkwill F. Cancer-related inflammation. Nature. 2008; 454:436–444. [PubMed: 18650914]

112. Leimgruber A, Berger C, Cortez-Retamozo V, Etzrodt M, Newton AP, Waterman P, Figueiredo JL, Kohler RH, Elpek N, Mempel TR, Swirski FK, Nahrendorf M, Weissleder R, Pittet MJ. Behavior of endogenous tumor-associated macrophages assessed in vivo using a functionalized nanoparticle. Neoplasia. 2009; 11:459–468. 2 p following 468. [PubMed: 19412430]

113. Jarzyna PA, Skajaa T, Gianella A, Cormode DP, Samber DD, Dickson SD, Chen W, Griffioen AW, Fayad ZA, Mulder WJ. Iron oxide core oil-in-water emulsions as a multifunctional nanoparticle platform for tumor targeting and imaging. Biomaterials. 2009; 30:6947–6954. [PubMed: 19783295]

114. Medarova Z, Pham W, Farrar C, Petkova V, Moore A. In vivo imaging of siRNA delivery and silencing in tumors. Nat Med. 2007; 13:372–377. [PubMed: 17322898]

115. Yang L, Peng XH, Wang YA, Wang X, Cao Z, Ni C, Karna P, Zhang X, Wood WC, Gao X, Nie S, Mao H. Receptor-targeted nanoparticles for in vivo imaging of breast cancer. Clin Cancer Res. 2009; 15:4722–4732. [PubMed: 19584158]

116. Kelly KA, Setlur SR, Ross R, Anbazhagan R, Waterman P, Rubin MA, Weissleder R. Detection of early prostate cancer using a hepsin-targeted imaging agent. Cancer Res. 2008; 68:2286–2291. [PubMed: 18381435]

117. Ko HY, Choi KJ, Lee CH, Kim S. A multimodal nanoparticle-based cancer imaging probe simultaneously targeting nucleolin, integrin alphavbeta3 and tenascin-C proteins. Biomaterials. 2011; 32:1130–1138. [PubMed: 21071077]

118. Chen W, Jarzyna PA, van Tilborg GA, Nguyen VA, Cormode DP, Klink A, Griffioen AW, Randolph GJ, Fisher EA, Mulder WJ, Fayad ZA. RGD peptide functionalized and reconstituted high-density lipoprotein nanoparticles as a versatile and multimodal tumor targeting molecular imaging probe. FASEB J. 2010; 24:1689–1699. [PubMed: 20075195]

119. Cai W, Chen K, Li ZB, Gambhir SS, Chen X. Dual-function probe for PET and near-infrared fluorescence imaging of tumor vasculature. J Nucl Med. 2007; 48:1862–1870. [PubMed: 17942800]

120. Montet X, Funovics M, Montet-Abou K, Weissleder R, Josephson L. Multivalent effects of RGD peptides obtained by nanoparticle display. J Med Chem. 2006; 49:6087–6093. [PubMed: 17004722]

121. Mulder WJ, Strijkers GJ, Habets JW, Bleeker EJ, van der Schaft DW, Storm G, Koning GA, Griffioen AW, Nicolay K. MR molecular imaging and fluorescence microscopy for identification of activated tumor endothelium using a bimodal lipidic nanoparticle. FASEB J. 2005; 19:2008–2010. [PubMed: 16204353]

122. Lee HY, Li Z, Chen K, Hsu AR, Xu C, Xie J, Sun S, Chen X. PET/MRI dual-modality tumor imaging using arginine-glycine-aspartic (RGD)-conjugated radiolabeled iron oxide nanoparticles. J Nucl Med. 2008; 49:1371–1379. [PubMed: 18632815]

123. Gianella A, Jarzyna PA, Mani V, Ramachandran S, Calcagno C, Tang J, Kann B, Dijk WJ, Thijssen VL, Griffioen AW, Storm G, Fayad ZA, Mulder WJ. Multifunctional nanoemulsion platform for imaging guided therapy evaluated in experimental cancer. ACS Nano. 2011; 5:4422–4433. [PubMed: 21557611]

124. de Vries IJ, Lesterhuis WJ, Barentsz JO, Verdijk P, van Krieken JH, Boerman OC, Oyen WJ, Bonenkamp JJ, Boezeman JB, Adema GJ, Bulte JW, Scheenen TW, Punt CJ, Heerschap A, Figdor CG. Magnetic resonance tracking of dendritic cells in melanoma patients for monitoring of cellular therapy. Nat Biotechnol. 2005; 23:1407–1413. [PubMed: 16258544]

125. Lewin M, Carlesso N, Tung CH, Tang XW, Cory D, Scadden DT, Weissleder R. Tat peptide-derivatized magnetic nanoparticles allow in vivo tracking and recovery of progenitor cells. Nat Biotechnol. 2000; 18:410–414. [PubMed: 10748521]

126. Keliher EJ, Yoo J, Nahrendorf M, Lewis JS, Marinelli B, Newton A, Pittet MJ, Weissleder R. 89Zr-labeled dextran nanoparticles allow in vivo macrophage imaging. Bioconjug Chem. 2011; 22:2383–2389. [PubMed: 22035047]

127. Yoo H, Kim JW, Shishkov M, Namati E, Morse T, Shubochkin R, McCarthy JR, Ntziachristos V, Bouma BE, Jaffer FA, Tearney GJ. Intra-arterial catheter for simultaneous microstructural and molecular imaging in vivo. Nat Med. 2011; 17:1680–1684. [PubMed: 22057345]

128. van Dam GM, Themelis G, Crane LM, Harlaar NJ, Pleijhuis RG, Kelder W, Sarantopoulos A, de Jong JS, Arts HJ, van der Zee AG, Bart J, Low PS, Ntziachristos V. Intraoperative tumor-specific fluorescence imaging in ovarian cancer by folate receptor-alpha targeting: first in-human results. Nat Med. 2011; 17:1315–1319. [PubMed: 21926976]

129. Kircher MF, de la Zerda A, Jokerst JV, Zavaleta CL, Kempen PJ, Mittra E, Pitter K, Huang R, Campos C, Habte F, Sinclair R, Brennan CW, Mellinghoff IK, Holland EC, Gambhir SS. A brain tumor molecular imaging strategy using a new triple-modality MRI-photoacoustic-Raman nanoparticle. Nat Med. 2012; 18:829–834. [PubMed: 22504484]

130. Heidt T, Deininger F, Peter K, Goldschmidt J, Pethe A, Hagemeyer CE, Neudorfer I, Zirlik A, Weber WA, Bode C, Meyer PT, Behe M, von Zur Muhlen C. Activated platelets in carotid artery thrombosis in mice can be selectively targeted with a radiolabeled single-chain antibody. PLoS One. 2011; 6 e18446.

131. Jaffer FA, Nahrendorf M, Sosnovik D, Kelly KA, Aikawa E, Weissleder R. Cellular imaging of inflammation in atherosclerosis using magnetofluorescent nanomaterials. Mol Imaging. 2006; 5:85–92. [PubMed: 16954022]

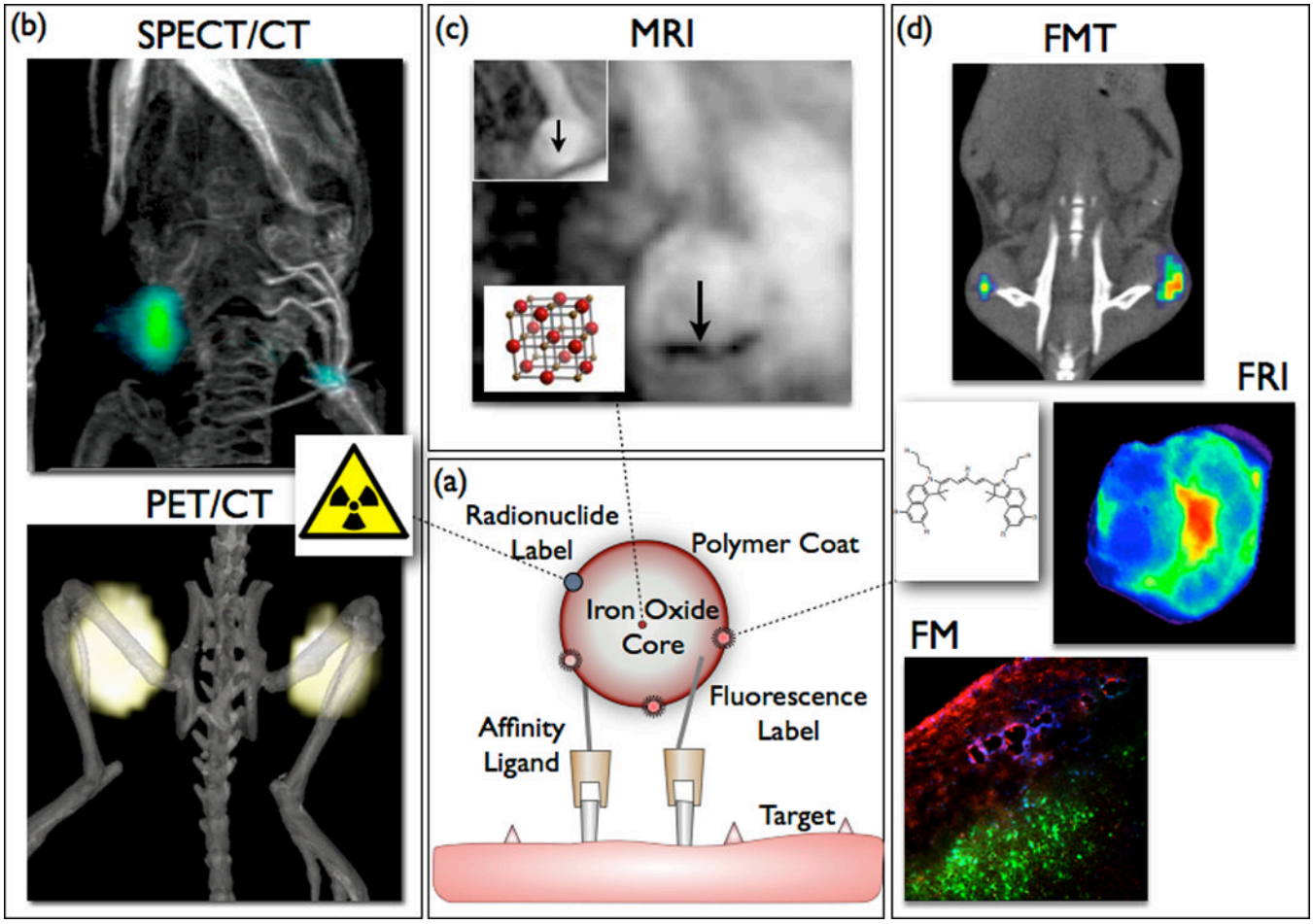


**Figure 1.**

Concept of a multimodal iron oxide core nanoparticle. **(a)** Iron oxide core is engulfed by a polymer shell (e.g. dextran). Amine groups bind affinity ligands and beacons for various imaging modalities (b–d). **(b)** Surface derivatization with radionuclides promotes nuclear imaging, e.g. positron emission tomography (PET, nanoparticles targeting tumor-associated macrophages)(86) or single photon emission computed tomography (SPECT, targeting activated platelets)(130). **(c)** Superparamagnetic iron oxide core cause signal decrease in $T_2$* weighted MRI (arrows show atherosclerotic plaque in apoE$^{-/-}$ mouse aorta)(131). **(d)** Fluorochromes attached to the nanoparticle surface enable optical imaging such as fluorescence molecular tomography (FMT), fluorescence reflectance imaging (FRI) or florescence microscopy (FM) (86). Images adapted with permission.

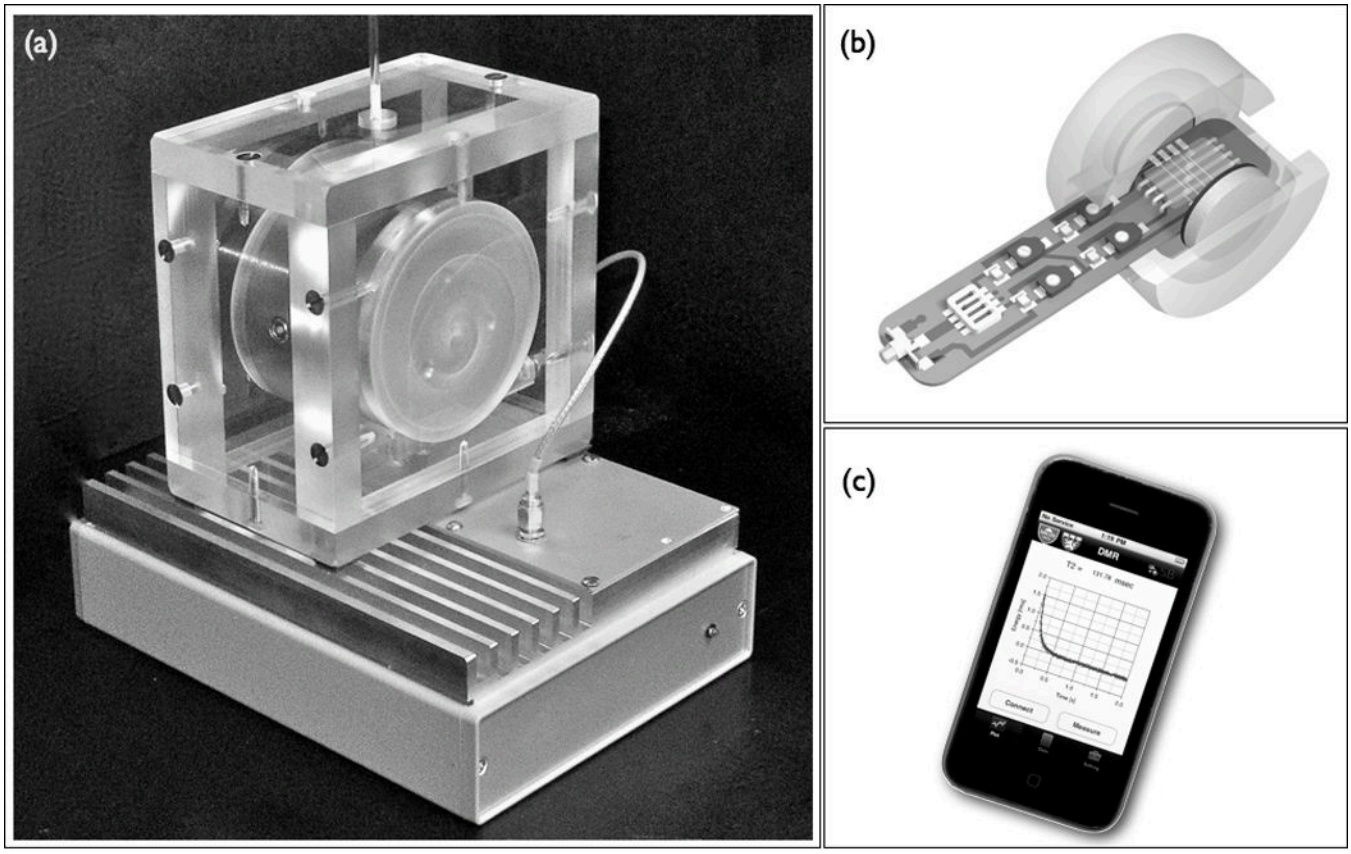


**Figure 2.**
Diagnostic magnetic resonance (DMR) applies iron oxide nanoparticles to detect analytes in blood, sputum, and biopsies with high sensitivity. (a) Miniaturized NMR as a point-of-care device. (b) Schematic of integrated DMR using a small permanent magnet. (c) DMR can be run by a smart phone application. Images adapted with permission (83).

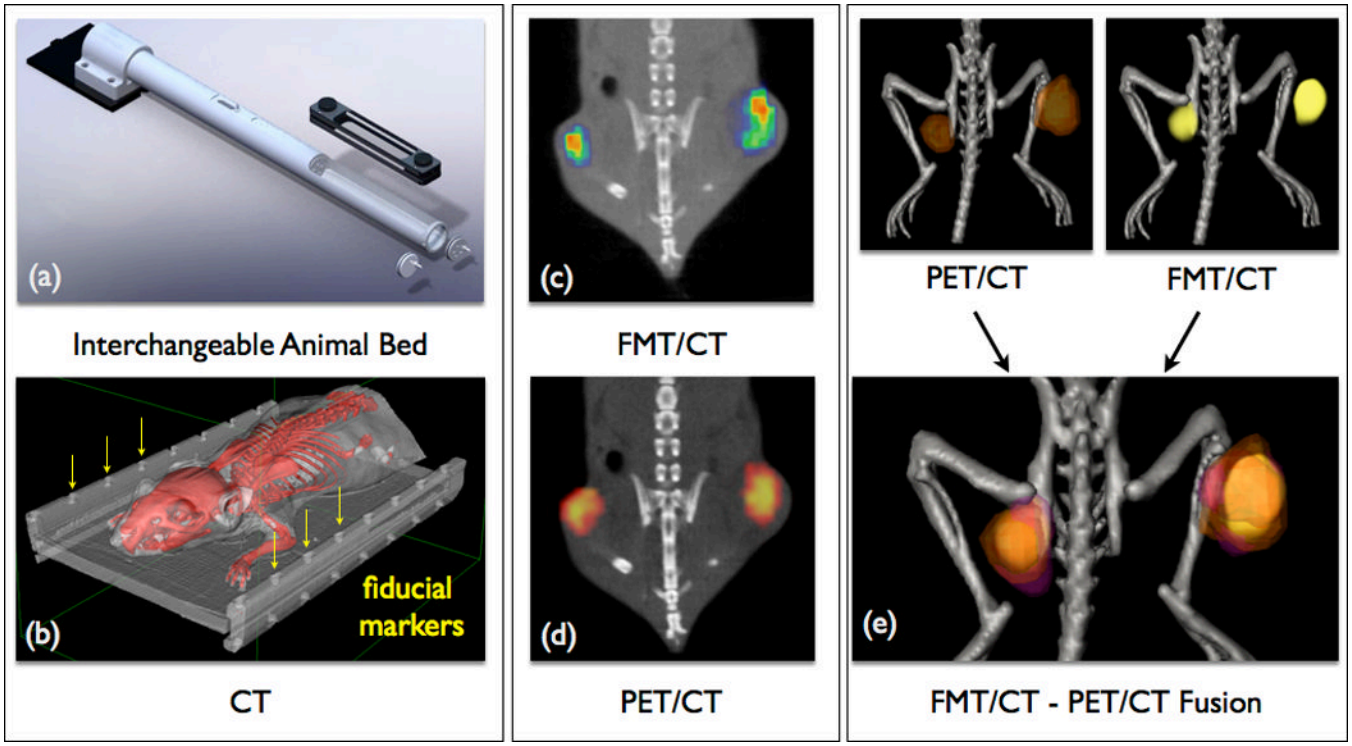


**Figure 3.**
Multimodality imaging combines complementary imaging techniques for optimizing sensitivity, temporal and spatial resolution and quantification. **(a)** Animal bed for transfer between imaging modalities (i.e. FMT, PET and MRI). **(b)** Fiducial markers (arrows) for image fusion are detected in all modalities. **(c)** FMT/CT image of tumor protease activity. **(d)** PET/CT image of phagocyte activity after co-injection of $^{64}$Cu-CLIO in the same mouse. **(e)** FMT-PET/CT image fusion integrates phagocyte and protease activity data (86). Images adapted with permission.

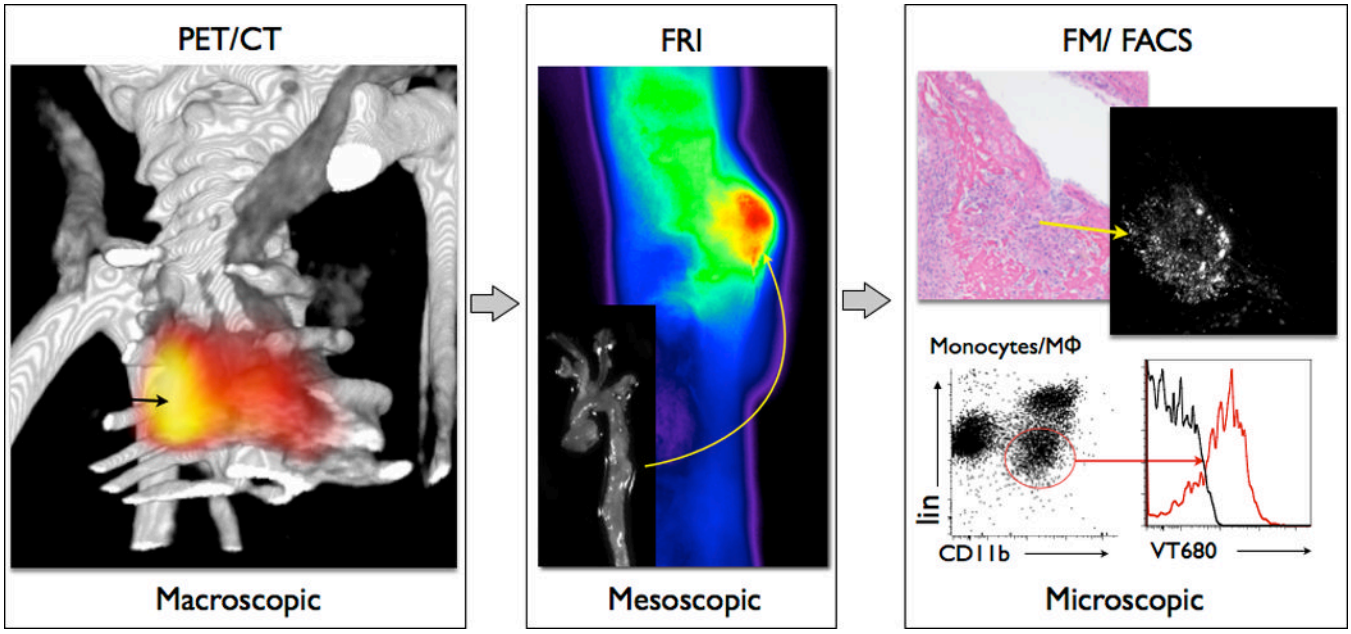


**Figure 4.**

Multiscale experiment with $^{18}$F-CLIO-VT680 in a murine model for aortic aneurysm (46). **Macroscopic:** Non-invasive PET/CT shows signal in the aneurysmatic thoracic aorta. **Mesoscopic:** Fluorescence reflectance imaging (FRI) of the excised aorta indicates specific nanoparticle uptake in aortic aneurysm with higher resolution. **Microscopic:** Fluorescence microscopy (FM) and flow cytometry (FACS) co-localize nanoparticles with macrophages in the aortic wall (46). Images adapted with permission.